DNA Strand Exchange Mediated by the *Escherichia coli* RecA Protein Initiates in the Minor Groove of Double-Stranded DNA

Xiaohua Zhou and Kenji Adzuma*

The Rockefeller University, Box 256, 1230 York Avenue, New York, New York 10021

Received December 6, 1996; Revised Manuscript Received February 6, 1997[⊗]

ABSTRACT: The *Escherichia coli* RecA protein can recognize sequence homology between a single-stranded DNA (ssDNA) and homologous double-stranded DNA (dsDNA). One model for the homology recognition invokes a DNA triplex intermediate in which specific hydrogen bonds connect the ssDNA with groups in the major groove of dsDNA. Using photo-cross-linking methods, we have analyzed the arrangement of DNA strands after the local strand exchange. The results showed that the displaced strand sits in the major groove of the hybrid duplex product. This arrangement indicates that the ssDNA invades the minor groove of dsDNA and hence argues against the involvement of triplex intermediates. The results support an alternative model for the homology recognition that invokes melting of the dsDNA and annealing of the one strand to the invading ssDNA.

Homologous recombination is a ubiquitous biological process. In eukaryotic organisms, it is intimately associated with meiosis and sexual reunion, playing vital roles in the creation of new combinations of genetic traits. Homologous recombination occurs also during normal cell cycles, and the recombination machinery supports the repair of damaged DNA and is also involved in various types of gene expression and development.

An early step of homologous recombination involves a process by which two DNA molecules with similar, or homologous, sequences are aligned and the strands are exchanged between them. The RecA protein of *Escherichia coli* catalyzes this DNA strand-exchange reaction between single-stranded DNA (ssDNA)[1] and homologous double-stranded DNA (dsDNA) molecules [for reviews, see Kowalczykowski (1991), Kowalczykowski and Eggleston (1994), and West (1992)]. RecA is the best-studied member of the RecA/Rad51 family of proteins that exist not only in bacteria (Roca & Cox, 1990) but also in higher eukaryotes including human (Shinohara et al., 1993; Yoshimura et al., 1993). Despite its ubiquitous importance, however, many aspects of the molecular mechanism of the strand-exchange reaction are not understood.

In the DNA strand-exchange reaction, one strand of the dsDNA becomes base paired with the original ssDNA, producing a hybrid duplex molecule, and the other strand of dsDNA eventually becomes displaced. We define the nomenclature for the three DNA strands involved in the strand exchange reaction as follows. "Incoming" strand refers to the ssDNA substrate; "recipient" strand is the strand in the dsDNA substrate whose sequence is complementary to the incoming strand; "outgoing" strand refers to the other strand of the dsDNA whose sequence is identical to the incoming strand. Thus after strand exchange, the outgoing strand becomes a displaced strand, while the incoming and recipient strands form a hybrid duplex molecule.

The catalysis of DNA strand exchange occurs in three steps. The first step is the polymerization of RecA onto a ssDNA substrate in the presence of ATP, producing a filamentous nucleoprotein complex called the presynaptic filament (Honigberg et al., 1985; Tsang et al., 1985). For the complex to be competent in subsequent steps, the binding of ATP to RecA is essential. In the second step, the presynaptic filament captures a naked dsDNA molecule that contains a sequence homologous to the resident ssDNA. The resulting complex, which holds three DNA strands together, is called a synaptic complex. The last step is a release of the strand-exchange products, a displaced strand and the hybrid duplex molecule. This last step requires the hydrolysis of ATP (Menetski et al., 1990), although the product release is not the only step which involves ATP hydrolysis [for a review, see Cox (1994)]. The synaptic complex accumulates when ATP is replaced by a practically non-hydrolyzable analogue such as ATPγS. There may be more than one type of synaptic complexes; but in this article, what we refer to as the synaptic complex is the one made in the presence of ATPγS. As described below, at least this type of synaptic complex represents a reaction stage after local strand exchange and is thus a kind of product complex.

A central question in homologous recombination is the mechanism by which a sequence similarity between two DNA molecules is recognized. In the case of RecA, homology recognition occurs between ssDNA and dsDNA molecules. Two models, the melting−annealing model and the triplex model, have been proposed to explain homology recognition [for reviews, see Camerini-Otero and Hsieh (1993), Stasiak (1992), and Cox (1995)]. Both models assume that recognition depends on specific base pairing between an incoming ssDNA and the homologous dsDNA molecule. What distinguishes the two models is the type of base pairing. The melting−annealing model pictures that homology is recognized by Watson−Crick base pairing

* Corresponding author. Phone: (212) 327-7471. Fax: (212) 327-7183. E-mail: adzuma@rockvax.rockefeller.edu.

[⊗] Abstract published in *Advance ACS Abstracts,* April 1, 1997.

[1] Abbreviations: ssDNA, single-stranded DNA; dsDNA, double-stranded DNA; ATPγS, adenosine-5′-*O*-(3-thiotriphosphate); SANPAH, *N*-succinimidyl-6-(4′-azido-2′-nitrophenylamino)hexanoate; SDS, sodium dodecyl sulfate; PAGE, polyacrylamide gel electrophoresis; bp, base pair; DMS, dimethyl sulfate.

S0006-2960(96)03006-1 CCC: $14.00 © 1997 American Chemical Society

between incoming and recipient strands, the two strands that together form a hybrid duplex molecule. Thus DNA synapsis and exchange of DNA strands are mechanistically coupled in this model, and the original base pairs must be broken for this type of homology recognition to occur. In the triplex model, non-Watson−Crick base pairing is responsible for homology recognition. Through specific hydrogen bonds, the non-Watson−Crick pairing connects an incoming ssDNA molecule to the homologous dsDNA molecule which retains the original Watson−Crick base pairs. The triplex model therefore postulates, as an intermediate of recombination, a triplex DNA that contains base triads. This putative recombination triplex has been named the R-DNA (Camerini-Otero & Hsieh, 1993).

We emphasize here that the R-DNA would have to be a novel structure that necessarily differs from canonical nucleic acid triplexes [for a review, see Frank-Kamenetskii and Mirkin (1995)]. First, R-DNA must be able to form with essentially any arbitrary sequence, whereas the formation of canonical triplexes requires a homopurine run in the dsDNA. Second, in R-DNA, the polarity of the third strand (i.e., incoming strand) must run in parallel to that of the identical strand (i.e., outgoing strand) in the Watson−Crick paired duplex. In canonical triplexes, however, the relative polarity of a pair of "like" strands is anti-parallel (Beal & Dervan, 1991; Moser & Dervan, 1987).

Does R-DNA exist? There is circumstantial evidence that it may (Hsieh et al., 1990; Rao et al., 1991, 1993; Shchyolkina et al., 1994). Some studies (Chiu et al., 1993; Rao & Radding, 1994), however, suggest that the R-DNA might be the one that forms after local strand exchange, i.e., a "post-exchange" triplex in which the outgoing strand is hydrogen bonded to the major groove of the hybrid duplex product. Relevance of this putative, post-exchange triplex to the mechanism of homology recognition is not clear. Attempts to detect "pre-exchange" R-DNA have so far produced negative results. We have examined the base-pairing status of the three DNA strands within the synaptic complex made in the presence of ATPγS, using chemical reagents whose reactivity toward DNA bases depends on their base-pairing status (Adzuma, 1992). The results did not reveal any base triads and instead were indicative of the products of strand exchange. On the basis of the photo-cross-linking results using a psoralen derivative, Jain et al. (1995) have also concluded that DNA strands within the synaptic complex appear to adapt the post-strand-exchange configuration, at least in the presence of ATPγS. Podyminogin et al. (1995) have analyzed the DNA structure within the synaptic complex by a chemical cross-linking technique and saw no evidence for base triads. With a general caveat of negative results in mind, the results of these studies suggest that R-DNA, as an intermediate in homology recognition, either does not exist or exists only transiently.

The issue of whether R-DNA exists only transiently or not at all can be approached from a different perspective. Several models have been proposed for the possible base-triad schemes of R-DNA (Hsieh et al., 1990; Rao et al., 1993; Zhurkin et al., 1994). In these schemes, the third strand is always placed in the major groove of dsDNA. This placement reflects the fact that the major groove has a much greater potential for distinguishing different base pairs than does the minor groove. The triplex model thus predicts that the incoming strand invades the major groove of its target

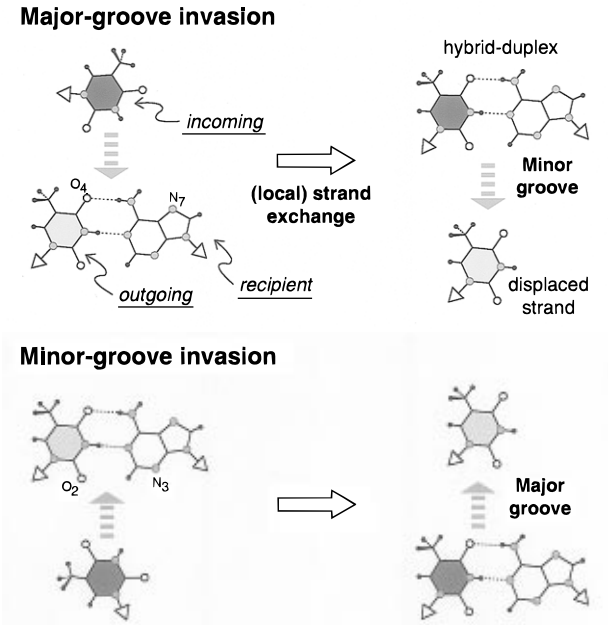

FIGURE 1: Two models for strand invasion. (Upper Panel) Major-groove invasion model; strand invasion from this groove leads to the displacement of outgoing strand into the minor groove of the hybrid duplex product. (Lower Panel) Minor-groove invasion model; after strand exchange, the locally displaced strand would be positioned in the major groove of the hybrid duplex product. Arrowheads attached to each base indicate a glycosyl bond pointing to the deoxyribose.

dsDNA. The melting−annealing model does not favor one particular groove over the other.

In this study, using DNA−DNA photo-cross-linking methods, we have examined the topography of the three DNA strands in a post-strand-exchange synaptic complex made in the presence of ATPγS. Our results indicate that, in this complex, the locally displaced strand sits in the major groove of the hybrid duplex product. This topography indicates that strand invasion occurs in the minor groove of the original dsDNA molecule (Figure 1). Our results thus not only support the conclusion of earlier studies (Baliga et al., 1995; Podyminogin et al., 1995) but also argue strongly against the triplex formation as the mechanism for homology recognition.

EXPERIMENTAL PROCEDURES

DNA. Sequences of the oligos used in this study are shown in Figure 2b. These oligos were synthesized on a DNA synthesizer and, except for the short (16-mer) hybridization probes, further purified by urea−polyacrylamide (sequencing) gel electrophoresis. Oligo 1 (or its photoreactive derivative, oligo 1XL) was annealed with oligo 2 (or oligo 2XL) to make a dsDNA substrate. After thermal annealing, NaCl was added to the sample to a final concentration of 150 mM, which was then passed through a nylon membrane filter using microfiltration centrifuge tubes (MicroFuge 0.22 μm, MSI). This procedure removed most of the un-annealed ssDNA species.

Unless otherwise noted, DNA concentrations are expressed in terms of the nucleotide concentration and were calculated from the absorbance at 260 nm using nominal extinction coefficients of 10 000 and 6 700 M^{-1} cm^{-1} for ssDNA and dsDNA, respectively. Some oligos were labeled with [^{32}P] at the 5′-ends, using ATP-[γ-^{32}P] and T4 polynucleotide

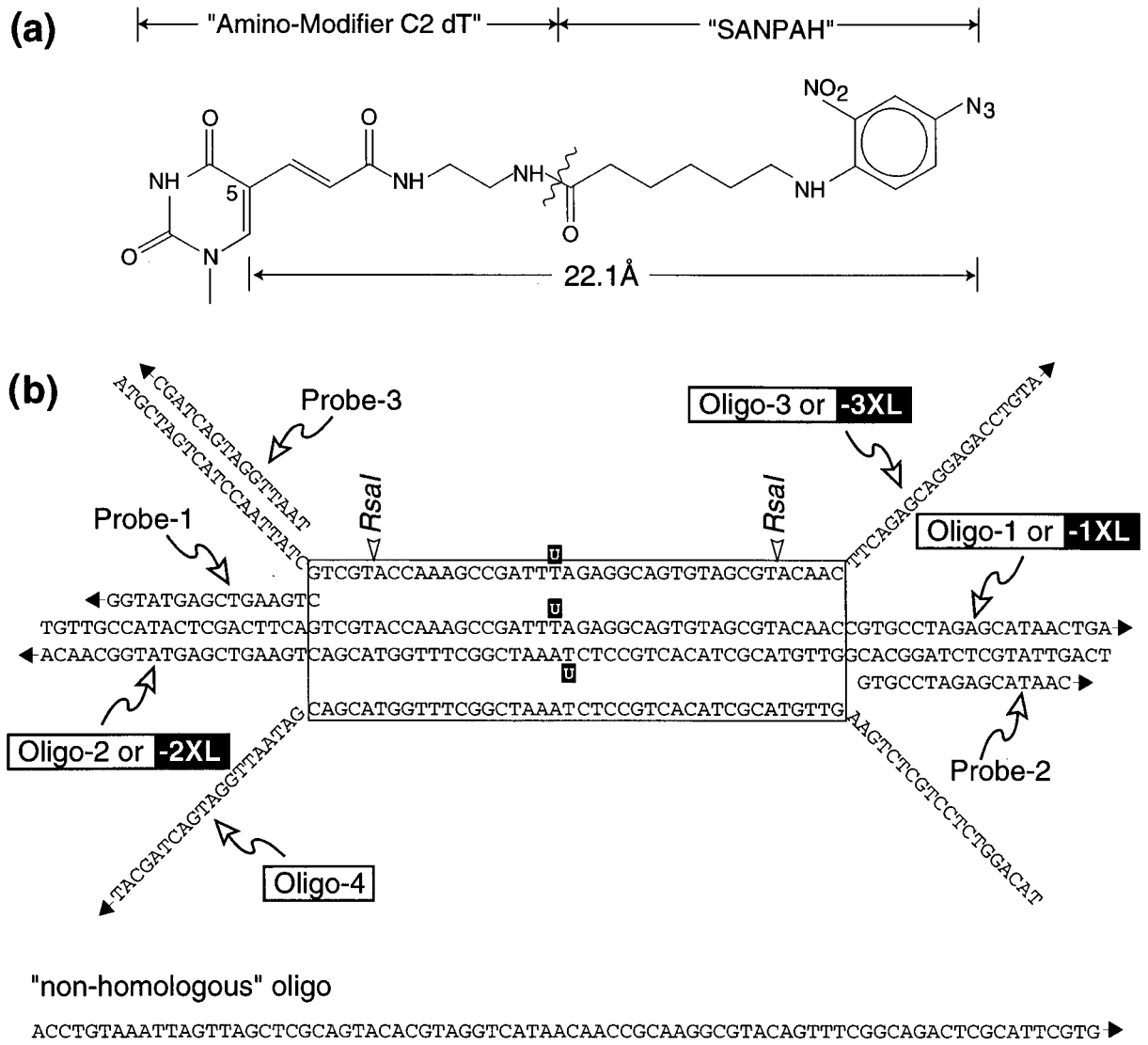

FIGURE 2: DNA substrates. (a) Structure of the photo-reactive base, dU*. The photo-reactive group, nitrophenyl azide, is attached to C-5 of uracil via a flexible linker. The photo-reactive oligo was synthesized by reacting an oligo containing an amino-modified deoxyuridine, "Amino-Modifier C2 dT," with a hetero-bifunctional cross-linker, "SANPAH"; the junction of this coupling is indicated by a wavy line. (b) DNA oligos. The 5′−3′ polarities of the oligos are indicated by arrows at one end of each sequence. Oligos 1−4 (80-mers) were used as DNA substrates in the DNA synapsis reaction. The suffix "XL" is attached to the names of photo-reactive oligos that contain a dU* in place of thymine; the position of dU* in each sequence is indicated by a shadowed "U" ("U" in a filled rectangle). The names of these photo-reactive oligos are also highlighted (i.e., white on black) in this and other figures. Oligo 1 (or 1XL) and oligo 2 (or 2XL) were annealed to make a dsDNA substrate; oligo 3 (or 3XL) and oligo 4 were used as ssDNA substrates. The region of homology is enclosed by a rectangle and contains two *Rsa*I restriction sites as indicated. Probes 1−3 are hybridization probes for oligos 1−3, respectively. The sequence of an 80-mer non-homologous ssDNA used throughout this study as a control is shown at the bottom.

kinase. After phosphorylation, free ATP was removed using a spin-column (Quick Spin G-25, Boehringer Mannheim) and the removal was confirmed by thin-layer chromatography. To prepare the oligo stock with a defined specific activity, we mixed the [^{32}P]-labeled oligo with an excess (at least 5-fold) known amount of the same but unlabeled oligo.

Proteins. RecA was purified from the overproducing strain JC12772 constructed by Uhlin and Clark (1981), according to the method developed by Cotterill et al. (1982) with minor modifications. The final fractions were dialyzed against the RecA dilution buffer containing 20 mM Tris-acetate (pH 7.5 at 1 M at room temperature), 0.1 mM EDTA, 1 mM dithiothreitol, and 10% (v/v) glycerol. The RecA concentration was determined from the absorbance at 278 nm in the RecA dilution buffer, using an extinction coefficient of 2.16×10^4 M^{-1} cm^{-1} (Kuramitsu et al., 1981). Sources of other proteins used in this study were as follows: restriction enzymes and T4 polynucleotide kinase, New England Biolabs; calf thymus terminal deoxynucleotidyl transferase, GIBCO-BRL.

Preparation of Photo-Reactive Oligos. To synthesize the photo-reactive oligos, we first incorporated, at a unique position in the sequence, a modified deoxyuridine residue carrying a primary amino group ("Amino Modifier C2 dT", Glen Research; see Figure 2a). The amino-modified oligos were reacted with a hetero-bifunctional cross-linker, "SANPAH" (Pierce; see Figure 2a). The SANPAH carries, at one end, the *N*-hydroxy succinimide (NHS) ester which reacts with primary amines and, at the other end, a photo-reactive nitrophenyl azido group. The coupling conditions were 0.5−1.0 μM (in molecules) of DNA oligos in 40 mM sodium carbonate buffer, pH 9, 60% (v/v) dimethyl sulfoxide, and 10−20 mM SANPAH, for 2 h at 30 °C. The NHS group leaves during the coupling. The reaction was quenched by

adding glycine to a final concentration of 100 mM, and the conjugated oligos were purified by two rounds of ethanol precipitation.

Efficiency of the SANPAH coupling was determined as follows. The coupled oligo was first annealed to its complementary strand and digested with *Rsa*I (see Figure 2b for the *Rsa*I positions). The DNA fragments were then labeled at the 3′-ends using α-[^{32}P]-dideoxyATP and terminal nucleotidyl transferase. This procedure generates six [^{32}P]-labeled strands (four 25-base long strands and two 30-base long strands; see Figure 2b) which can be separated by sequencing gel electrophoresis. Efficient coupling of SANPAH slightly retards the electrophoretic mobility of one of the two 30-base long strands, relative to the uncoupled strand. By this protocol, we estimated that the efficiency of SANPAH coupling was routinely about 90% under the conditions described above. The purpose of *Rsa*I digestion was to shorten the DNA segment conjugated with SANPAH; without shortening, a small change in electrophoretic mobility (equivalent to about one-base difference in sequencing gel electrophoresis) was difficult to detect.

DNA Synapsis Reactions. The standard reaction mixture to make the synaptic complex contained three kinds of DNA: 1.6 μM (20 nM in molecules) of 80-mer incoming ssDNA, 1.6 μM (10 nM in molecules) of 80-bp homologous dsDNA target, and 50 μM pUC19 DNA linearized by *Sca*I. This pUC19 DNA is not homologous to the incoming ssDNA and was included to reduce the nonspecific binding of RecA to the 80-bp dsDNA target. The reaction buffer consisted of 40 mM Tris-acetate (pH 7.5), 100 mM potassium acetate, 9 mM magnesium acetate, 1 mM dithiothreitol, 250 μM ATPγS, and 100 μg of bovine serum albumin (BSA) per mL. The reaction was initiated by adding RecA to a final concentration of 1.0 μM and the mixture was incubated at 37 °C for 2−3 h. The dsDNA target contains two *Rsa*I sites (see Figure 2b) and the formation of the synaptic complex prevents these sites from digestion by *Rsa*I. Under our reaction conditions, about half of the homologous dsDNA target became resistant to the *Rsa*I digestion.

UV Photo-Cross-Linking. Photo-cross-linking was carried out with a hand-held long-wavelength UV lamp (UVP model UVL-56, 366-nm maximum). Optimal photolysis of nitrophenyl azide occurs at 320−350 nm (Lewis et al., 1977). To cut off the short-wavelength UV which could photodamage RecA and/or DNA, the lamp was covered with a polystyrene plate (plastic cover of microtiter dish or Petri dish) whose transmittance was about 60% at 366 nm and almost zero at 260 nm (measured with a spectrophotometer). Samples containing the synaptic complex were spotted on parafilm in 25-μL aliquots and then irradiated with the lamp for 2−3 min at a distance of 5 cm; the intensity of UV under this condition was 800 μW/cm^2 at 360 nm.

Analysis of the Cross-Linked Products Involving a Photo-Reactive Incoming Strand. The synaptic complex was made between 1.0 pmol (in molecules) of oligo 3XL and 0.5 pmol of a dsDNA target comprising oligo 1 and oligo 2, in a total volume of 50 μL. After UV irradiation, the SDS was added to the samples to a final concentration of 0.25% and they were digested with Protease-K (100 μg/mL, final) at 37 °C for 15 min. The DNA was collected by ethanol precipitation, resuspended, and divided into aliquots, each of which was run separately on a 6% sequencing gel casted on a mini-gel apparatus (0.5-mm thickness × 7-cm height). The DNA molecules in each gel were then electrotransferred to a membrane filter (Zeta-Probe, Bio-Rad). The membrane was subsequently irradiated with short-wavelength UV lamps (Strata-linker, Stratagene) to immobilize the DNA. The strand composition of the cross-linked products were analyzed by hybridization with [^{32}P]-labeled probes specific to each strand. For the conditions of pre-hybridization and hybridization, we essentially followed the manual supplied with the membrane.

Chemical Probing of the Synaptic Complex. The procedure was similar to that described in Adzuma (1992). The synaptic complex was made under the standard condition (200 μL in total), using a dsDNA substrate labeled with [^{32}P] at the 5′-end of either strand. After a 3-h incubation at 37 °C, 12 μL of *Rsa*I (10 units/μL) was added to the reaction mixture and incubation was continued for another 15 min. At this point, 5 μL of 10% DMS (diluted in ethanol) or 5 μL of 100 mM $KMnO_4$ (freshly dissolved in water) was added to each sample, followed by additional incubation at 37 °C for 2 min. The reaction was quenched by adding 50 μL of ice-cold "DMS stop buffer" of Maxam and Gilbert (1980) and 750 μL of ethanol chilled at −20 °C. The DNA was collected by centrifugation, suspended with 250 μL of 0.3 M sodium acetate (pH 7.0) on ice, and precipitated again with ethanol. The DNA samples were then fractionated on a non-denaturing polyacrylamide gel. The band corresponding to the intact 80-bp fragment was identified by a brief autoradiography, and the DNA fragment was extracted from the gel slice by the conventional "crush and soak" method.

After the gel purification, the $KMnO_4$-modified fragment was cleaved by hot piperidine (1 M piperidine at 90 °C for 30 min). The DMS-modified fragment was suspended with a mixture of 15 μL of water and 5 μL of butanol on ice. To each sample was added 20 μL hydrazine, and the mixture was kept on ice for 4 min. The reaction was quenched by adding 200 μL of ice-cold "hydrazine stop buffer" of Maxam and Gilbert (1980) and 750 μL of chilled ethanol. After pelleting, suspension, and one more round of ethanol precipitation, the sample was treated with hot piperidine. This brief hydrazine treatment enhances the piperidine cleavage of N-3-methylated cytosine (Cowing et al., 1989; the protocol cited as personal communication from K. Kirkegaard).

We note that methylation by DMS is difficult to quench thoroughly. Therefore, after addition of the DMS stop buffer, the samples should be processed at a low temperature and as quickly as possible, to minimize the methylation that could occur after the destruction of the synaptic complex. In our hands, when DMS was added immediately after addition of the DMS stop buffer, the degree of guanine methylation was routinely 10−20% of that found with the normal order of addition.

RESULTS

The groove into which the incoming strand invades for strand exchange.

Because the two sides of dsDNA, the major and minor grooves, are distinct, there are two non-equivalent ways to initiate strand exchange. The incoming strand might invade the major-groove side of the target dsDNA molecule (Figure 1, upper panel), or it might invade the opposite minor-groove side (lower panel). Such intrinsic asymmetry in the initiation of three-strand exchange would lead to asymmetry in the

topography of strand-exchange products. If strand invasion occurs in the major groove of the dsDNA substrate, the outgoing strand should be displaced into the minor groove of the hybrid duplex product. In the case of minor-groove invasion, the outgoing strand should be located in the major groove of the hybrid duplex molecule after strand exchange.

The triplex model for homology recognition postulates the existence of a "recombination triplex" or R-DNA in which specific hydrogen bonds connect the bases of the incoming strand to hydrogen-bond donors and acceptors in the major groove of the target dsDNA [for a review, see Camerini-Otero and Hsieh (1993)]. Thus the triplex model implies the major-groove invasion, to the extent that a triplex with the third strand in the minor groove is unprecedented. The melting−annealing model for homology recognition has no intrinsic preference for either groove in the initiation of strand invasion. Note that the major or minor groove in this context does not infer the width of the groove, but merely refers to a particular edge of bases, each defined by distinctive functional groups. The minor-groove edge of a base is defined as the one which would be seen in the minor groove in B-DNA and is characterized by the purine N-3 and the pyrimidine O-2; the major-groove edge is characterized by the purine N-7, thymine O-4, and cytosine N-4 (see Figure 1).

Experimental Strategy. To distinguish between the major-groove and minor-groove invasion models, we synthesized a set of photo-reactive DNA oligonucleotides (oligos), each carrying a single photo-cross-linker conjugated to the major-groove edge of a uracil residue. The synthesis was done by first incorporating a modified uracil residue which carries a primary amino group and then reacting this oligo with a hetero-bifunctional cross-linker SANPAH. In the resulting photo-reactive uracil residue (Figure 2a; referred to as dU*), an arylazido group is attached to the C-5 position of uracil via a flexible linker. The photo-reactive group should therefore be positioned in the major groove if the oligo that carries it becomes part of a dsDNA molecule. The DNA synapsis reaction in this study consists of an 80-mer ssDNA substrate and an 80-bp dsDNA substrate. Figure 2b summarizes the names and sequences of each DNA species. The region of homology, indicated by a rectangle, is restricted to the middle 40-bp sequence. The 20-bp of non-homology at both ends prevents a locally displaced strand from completely escaping from the synaptic complex.

Three sets of DNA substrates were used in this study. In each set, only one of the three DNA strands (incoming, recipient, or outgoing) contained the photo-reactive dU* residue. The [^{32}P] label was also placed on only one of the three strands, normally on the same strand as dU* unless otherwise noted. We formed the synaptic complex using each of these three substrate sets, irradiated the complex with UV to induce photo-cross-linking, and then analyzed the cross-linking patterns. Our questions were as follows: (1) Can the cross-linker attached to the major groove of a particular strand cross-link to any other strand within the synaptic complex? (2) If it does cross-link, then to which DNA strand(s)?

The rationale for these experiments is as follows. Suppose that the photo-cross-linker is attached to the incoming strand (in Figure 1, this means that the methyl group of thymine on the incoming strand is replaced with the cross-linker). The major-groove invasion model predicts that, in the synaptic complex (i.e., after local strand exchange), the outgoing strand would be located in the minor groove of the hybrid duplex product. In this case, a cross-linker attached to the major-groove edge of a base in the incoming strand should not be able to cross-link to the outgoing strand, because the cross-linker and the outgoing strand would be located in opposite grooves of the hybrid duplex molecule. By contrast, according to the minor-groove invasion model, the photo-reactive incoming strand could cross-link to the outgoing strand after strand-exchange, because the cross-linker and the outgoing strand would reside in the same groove of the hybrid duplex product. The same predictions hold if the cross-linker is placed on the recipient strand; i.e., the major-groove invasion model predicts that a cross-linker attached to the major-groove edge of a base in the recipient strand should not be able to cross-link to the outgoing strand within the synaptic complex, while the minor-groove invasion model predicts that it could. In other words, if the cross-linker on either the incoming or the recipient strand cross-linked to the outgoing strand within the synaptic complex, then these results would contradict the prediction of the major-groove invasion model. As described below, these results are precisely what we obtained.

A Photo-Reactive Incoming Strand Can Cross-Link to the Outgoing Strand within the Synaptic Complex. We first show the results using a photo-reactive incoming strand. The synapsis reaction was carried out using a [^{32}P]-labeled, photo-reactive ssDNA substrate and the homologous dsDNA substrate that was neither [^{32}P]-labeled nor photo-reactive (Figure 3a). After synapsis, the samples were irradiated by UV and the cross-linking patterns analyzed by SDS−PAGE. As shown in Figure 3b, the irradiation produced a discrete band (indicated by an arrowhead) that was resistant to digestion with Protease-K (compare lane 1 with lane 2). Production of this band required the presence of RecA, ATPγS, UV irradiation, coupling of photo-cross-linker, and homology (lanes 3−7). We therefore concluded that this band represents azido-driven DNA−DNA cross-linking within the synaptic complex.

To which DNA strand in the synaptic complex did this photo-reactive incoming strand cross-link? To answer this question, we prepared the cross-linked products using the same photo-reactive, but unlabeled, incoming strand. After cross-linking, the samples were separated by urea−polyacrylamide (sequencing) gel electrophoresis and the DNA was transferred to membrane filters. Each filter was then subjected to hybridization with a [^{32}P]-labeled probe specific to the incoming, recipient, or outgoing strand. To evaluate the hybridization stringency, each filter also contained an equal amount of the three DNA oligos that had been used as incoming, recipient, and outgoing strands. As shown in Figure 3c, the resulting autoradiograms revealed that the majority (∼80%) of cross-linked products involved the outgoing strand as the target of cross-linking; a smaller (∼20%) fraction of cross-linked products involved the recipient strand as the target.

A Photo-Reactive Recipient Strand, but Not the Outgoing Strand, Can Produce Cross-Linked Products within the Synaptic Complex. The next two sections describe experiments in which the cross-linker was placed in one of the strands in the dsDNA target. Figure 4a summarizes the four combinations of DNA substrates used in these experiments. In combinations 1 and 2, the cross-linker was attached to

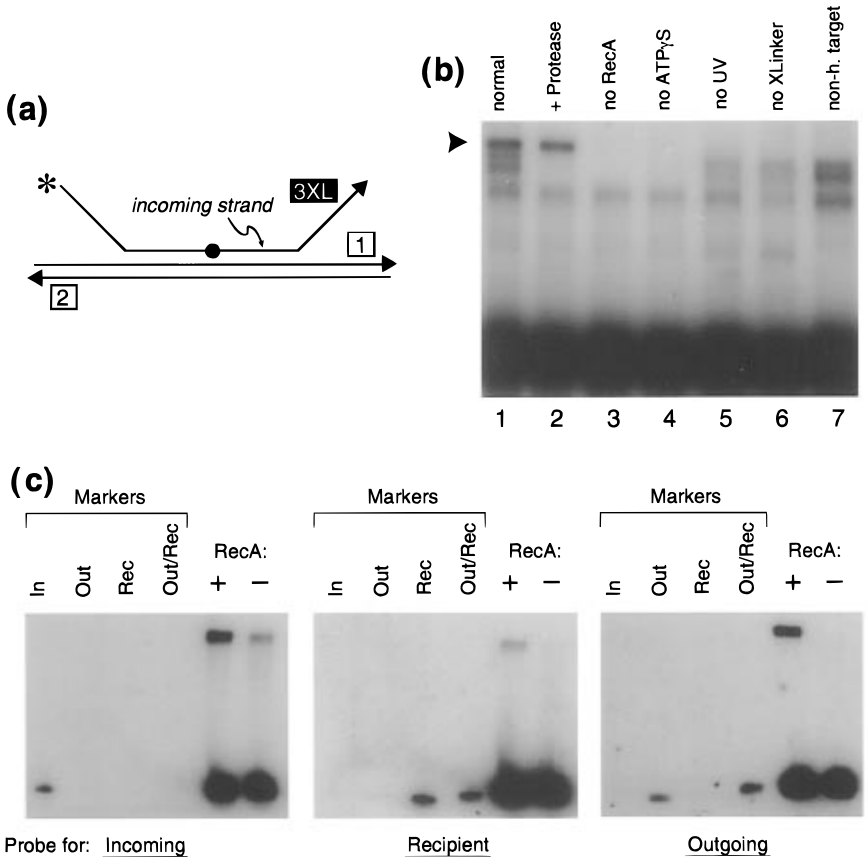

FIGURE 3: Photo-cross-linking results with the cross-linker on incoming strand. (a) Substrate combination. DNA strands are shown by arrows, the directions of which indicate the 5′−3′ polarities. Numbers in rectangles refer to the names of oligos (e.g., "1" refers to oligo 1); the highlighted name (3XL in this case) means the oligo is photo-reactive. Cross-linker is shown by a ball, and [^{32}P] label is shown by an asterisk. (b) Photo-cross-linking results. After the synapsis reaction, the samples were irradiated by UV and the cross-linking patterns were analyzed by 10% SDS−PAGE, followed by autoradiography. Lanes 1 and 2: results of photo-cross-linking without (lane 1) and with (lane 2) Protease-K treatment after cross-linking. Lanes 3−7: control reactions without RecA (lane 3); without ATPγS (lane 4, ADP was added instead); without UV irradiation (lane 5); using an incoming oligo not yet coupled with the cross-linker (lane 6); and using a non-homologous 80-bp dsDNA target (lane 7). (c) Differential hybridization analyses. DNA synapsis and UV irradiation were carried out as in panel b but with unlabeled incoming strand. After the irradiation, samples were treated with Protease-K and divided into aliquots, each of which was run on a sequencing gel (6%) separately. The DNA in the gel was then electrotransferred onto a membrane filter and immobilized by UV cross-linking (see Experimental Procedures). Each filter was hybridized with a [^{32}P]-labeled probe specific to incoming (probe 3 in Figure 2b), recipient (probe 2), or outgoing (probe 1) strand, as indicated at bottom. Lanes (from left to right): 0.1 pmol (in molecules) of each of the oligos used as incoming (In, oligo 3XL), outgoing (Out, oligo 1), and recipient (Rec, oligo 2) strands; 0.1 pmol of target dsDNA (Out/Rec, oligo 1/oligo 2); results of synapsis cross-linking reactions with (+) and without (−) RecA. In the panel probed for the incoming strand, there was a faint band even in the negative control (−RecA) which co-migrated with the cross-linked product. This species involves only the incoming strand and the same band was seen even without UV irradiation (not shown); the band most likely reflects a cross-linking between two molecules of the photo-reactive oligo which might have occurred during its preparation.

the "top" strand of the dsDNA, while in combinations 3 and 4, it was attached to the "bottom" strand. To form the synaptic complex, each dsDNA substrate was mixed with a homologous ssDNA molecule that was either identical or complementary to the central portion of the photo-reactive strand. For example, in combination 1 (see Figure 4a) we used an incoming strand which contained a sequence complementary to the photo-reactive strand. In this combination, the photo-reactive strand functions as the recipient strand. In combination 2, the same photo-reactive strand functions as the outgoing strand because the incoming strand was identical to the central portion of the photo-reactive strand.

The synaptic complex was formed using each of these substrate combinations with [^{32}P]-label on the photo-reactive strand and irradiated by UV, and the cross-linking patterns were analyzed by sequencing gel electrophoresis. Figure 4b shows the resulting autoradiograms. When the cross-linker was on the outgoing strand (see columns marked "Out"; i.e., combinations 2 and 4), we did not detect any significant cross-linking, compared to a control in which non-homologous ssDNA was used as the ssDNA substrate. By contrast, we observed efficient cross-linking with the photo-reactive recipient strand (see columns marked as "Rec"; combinations 1 and 3). The cross-linked product was resistant to protease digestion, and its formation required the presence of RecA, ATPγS, UV irradiation, coupling of cross-linker, and homology.

Both the top and bottom strands of the dsDNA target yielded the cross-linked product when these strands carried a cross-linker and functioned as a recipient strand, but neither strand produced cross-linked products when it acted as an outgoing strand. Thus the ability to cross-link depends solely on the function of the oligo in the DNA synapsis reaction and not on physical properties specific to individual oligos. We note that the cross-linker in these experiments was placed on what was originally a dsDNA molecule. It therefore supports some degree of DNA−DNA cross-linking even in

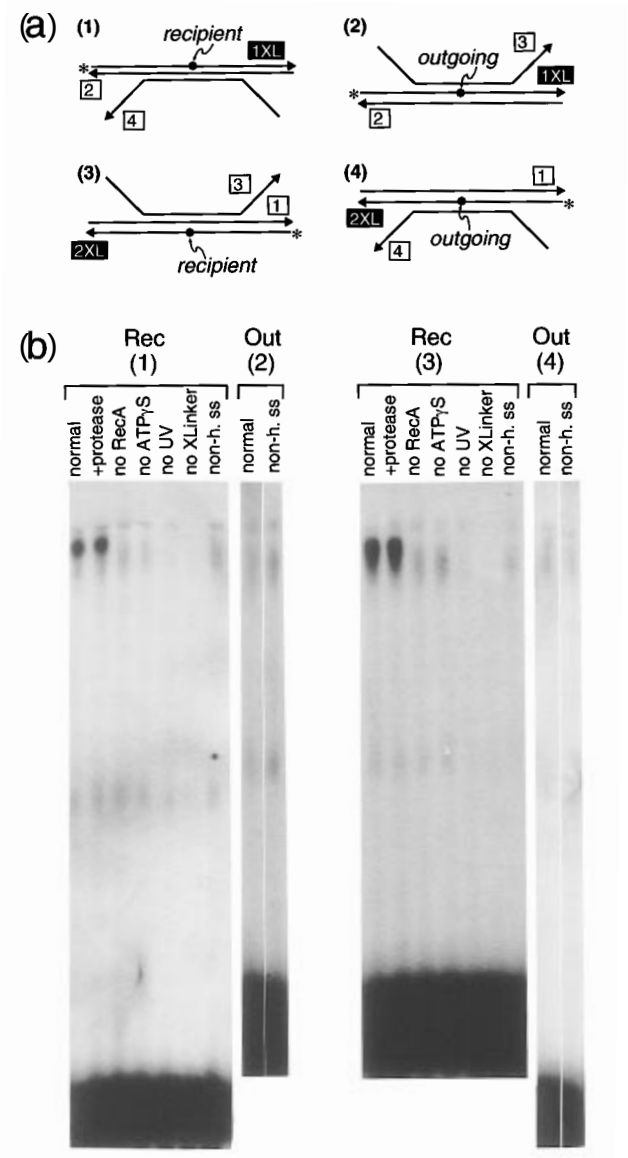

FIGURE 4: Cross-linking results with a photo-reactive dsDNA substrate. (a) Substrate combinations. In each combination, the cross-linker (indicated by a ball) and [^{32}P] label (an asterisk) are on the same strand; the function of this strand, either recipient or outgoing strand, is indicated. (b) Results of cross-linking. After the DNA synapsis, the samples were irradiated by UV and directly run on an 8% sequencing gel. The resulting autoradiograms are shown. Each column corresponds to the results with each substrate combination, 1−4, of panel a. The functional name of the photo-reactive, [^{32}P]-labeled strand is also indicated for each column; "Rec" and "Out" stand for recipient and outgoing strands, respectively. The label "non-h. ss" means non-homologous ssDNA used as the ssDNA substrate (negative control).

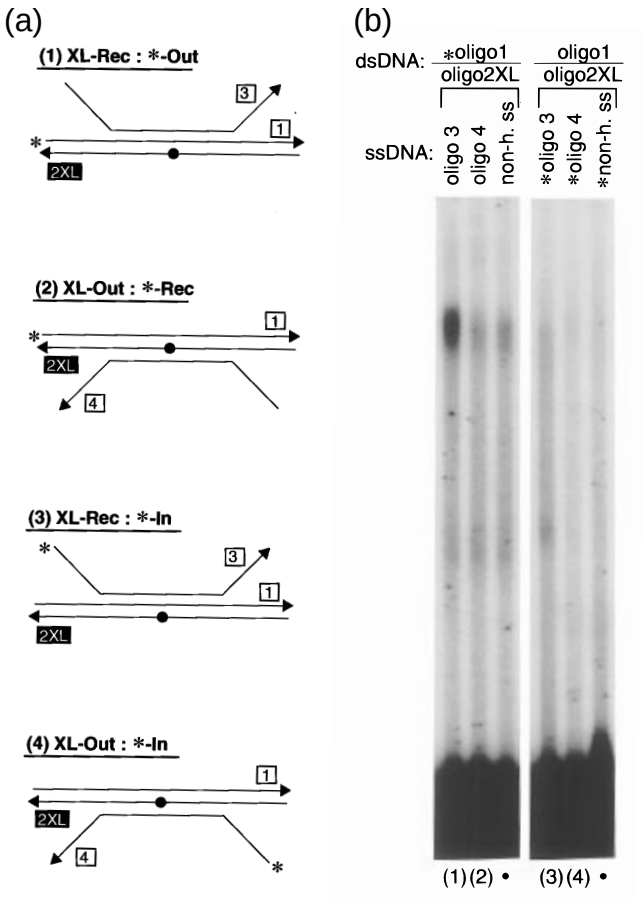

FIGURE 5: Target of cross-linking with a photo-reactive recipient strand. (a) Substrate combinations. Symbols are the same as in the previous figures. Placement of cross-linker and [^{32}P] label are indicated; for example in combination 1, "XL-Rec:*-Out" means that the cross-linker is on the recipient strand (Rec) and the [^{32}P] label is on the outgoing strand (Out). (b) Results of cross-linking. Autoradiogram of the analyses on an 8% sequencing gel. The oligo names of ssDNA and dsDNA substrates are shown at the top; except for negative controls in which a non-homologous oligo (non-h. ss) was used as the ssDNA substrate, the lane numbers correspond to the substrate combinations of panel a.

the absence of DNA synapsis, most likely involving the complementary strand as the target of cross-linking (for example, compare the lanes "no RecA" with "no UV" in Figure 4b). However, the degree of such synapsis-independent cross-linking was very low; the same photo-reactive strand supports much more efficient cross-linking when it acts as a recipient strand within the synaptic complex.

Primary Target of Recipient-Strand Cross-Linking Is the Outgoing Strand. To which DNA strand in the synaptic complex did the photo-reactive recipient strand cross-link? We initially attempted to answer this question by the same differential hybridization method described earlier. However, we did not detect any significant signal even with a probe for the photo-reactive oligo. These negative results, we reasoned, could be explained if the majority of the cross-linking were between the recipient (which had the cross-linker) and outgoing strands. These two strands are entirely complementary to each other. When cross-linked together, rapid annealing of these two strands would compete out the hybridization with a short probe.

Therefore we changed the experimental strategy and, instead of differential hybridization, placed the [^{32}P] label on each of potential target strands differentially (Figure 5a). The dsDNA substrate was identical among each substrate combination, consisting of a photo-reactive oligo and its non-photo-reactive complement. As the incoming strand, we used either oligo 3 or oligo 4; oligo 3 makes the photo-reactive strand function as the recipient strand and oligo 4 makes it function as the outgoing strand (negative control). The position of [^{32}P] label was then varied as indicated by asterisks in Figure 5a.

Figure 5b shows the photo-cross-linking results. Here, the most relevant comparison is between the results of combination 1 (dU* on recipient strand, [^{32}P] label on outgoing strand) and those of combination 3 (dU* on the same recipient strand, but the label on incoming strand). When

the label was on the outgoing strand, we clearly detected cross-linking (see lane labeled "1" at the bottom in Figure 5b). When the label was on the incoming strand, however, we did not see any band corresponding to the cross-linked product (see lane labeled "3"). By using a protocol described in Experimental Procedures (see "Preparation of Photo-Reactive Oligos"), we verified the existence of cross-linker in the dsDNA substrate used in combination 3; the negative results obtained with this substrate combination was therefore not a result of poor coupling of SANPAH (data not shown). Taken together, we conclude that the target of cross-linking with the photo-reactive recipient strand is primarily the outgoing strand, rather than the incoming strand.

Which Reaction Stage Do the Photo-Cross-Linking Patterns Represent? We have so far shown that our photo-cross-linker, when attached to either the incoming or recipient strand, cross-links primarily to the outgoing strand within the synaptic complex. As mentioned earlier (see "Experimental Strategy"), assuming that the cross-linking patterns we obtained represent a reaction stage after strand exchange, these results contradict predictions based on the major-groove invasion model, but not those based on the minor-groove invasion model. However, if the complex we analyzed somehow represents a pre-strand-exchange stage, the our results do not distinguish between the two models, because either model can in principle account for the observed cross-linking results. For example, before exchange, a photo-reactive incoming strand could conceivably cross-link to any strand including the outgoing strand, irrespective of the groove which it invades.

Previously, we (Adzuma, 1992) and others (Jain et al., 1995; Podyminogin et al., 1995) have shown that the synaptic complex made in the presence of ATPγS is a complex in which the strand exchange has already taken place. However, one must be cautious in applying these findings to the current study, because here we used DNA substrates to which we attached a bulky photo-cross-linker. Because our photo-reactive oligos support DNA synapsis as efficiently as normal oligos do (data not shown), we can at least conclude that attaching the photo-cross-linker does not cause any significant inhibition of overall DNA synapsis. However, what is critical in interpreting the photo-cross-linking patterns obtained in this study is not the overall synapsis efficiency but the local base-pairing status at or very near the position of dU*. This issue was addressed in the following experiments.

Attachment of the Photo-Cross-Linker Does Not Inhibit the Local Exchange of DNA Strands. The experimental strategy was the same as in Adzuma (1992). Namely, we made the synaptic complex using the dU*-containing oligo as one of the three functional DNA strands and then examined the reactivities of DNA bases within the complex toward dimethyl sulfate (DMS) and potassium permanganate ($KMnO_4$). As a reference, we carried out the same experiment with a regular oligo containing a thymine (T) residue in place of dU*. $KMnO_4$ oxidizes the C-5/C-6 π bond of T. Since this oxidation occurs by attack perpendicular to the pyrimidine ring, base stacking provides protection and normal dsDNA is insensitive to $KMnO_4$. When stacking interactions are disrupted, as in the melting of dsDNA, the susceptibility to $KMnO_4$ greatly increases (Iida & Hayatsu, 1971). DMS primarily methylates N-7 of guanine (G); it can also methylate, to a much lesser extent, N-3 of cytosine (C). This position, however, becomes accessible to DMS only when the C residue is not base paired, because the N-3 of C is involved in Watson−Crick base pairing.

Figure 6 shows the results of chemical probing analyses obtained with the synaptic complex involving a photo-reactive incoming strand (see the drawings at the top of Figure 6). By examining the electrophoretic mobility of the DNA segment to which the cross-linker was attached, we confirmed that essentially all the molecules of this incoming strand contained the cross-linker (data not shown; see Experimental Procedures). Figure 6a shows the reactivities of the outgoing strand, and Figure 6b shows those of the recipient strand. Within the synaptic complex, T residues in the outgoing strand show very high reactivities toward $KMnO_4$; the reactivities are highest at the center of homologous region and gradually decrease outward. By contrast, the $KMnO_4$ reactivities of the recipient strand tend to display a strong position dependence. These observations (Adzuma, 1992) were reproduced here (lanes "w/o XL" in columns "$KMnO_4$" of Figures 6a and 6b). More importantly, we observed virtually identical pattern of $KMnO_4$ reactivity even with the synaptic complex involving the dU*-containing incoming strand (lanes "w/XL"). Note that the position of one T residue on the outgoing strand (see panel a) coincides with the position of dU* (indicated by a thick arrow) on the incoming strand; a T residue on the recipient strand (panel b) is only one nucleotide away from the position of dU*. Even at these positions, we did not detect any significant change in $KMnO_4$ reactivities. DMS methylates N-7 of G in both outgoing and recipient strands within the synaptic complex; DMS also methylates C residues in the outgoing strand but not those in the recipient strand [see Adzuma (1992), and this study]. Again, we saw virtually no difference in DMS reactivity patterns between the complex made with a dU*-containing incoming strand and that made with a regular oligo; the closest C residues are five and two nucleotides away from the position of dU* in the outgoing and recipient strands, respectively.

Figure 7 shows the results of the same chemical probing analyses when the dsDNA substrate contained the cross-linker. The figure shows the DMS and $KMnO_4$ reactivities of the strand complementary to the dU*-containing strand. By using two ssDNA substrates as the incoming strand, we obtained the reactivity patterns corresponding to the outgoing (lanes labeled "Out") and recipient strands ("Rec"). In either strand, there was no discernible difference in reactivities between the synaptic complex made with the dU*-containing oligo (lanes labeled "w/XL") and the complex made with a regular oligo ("w/o XL").

DISCUSSION

Outgoing Strand Sits in the Major Groove of the Hybrid Duplex Product within the Synaptic Complex. In this study, we placed a photo-cross-linker in the major-groove edge of a DNA oligo and used this photo-reactive oligo as one of the three DNA strands to form the synaptic complex. Two series of experiments were carried out. In the first series, we irradiated the complex with UV and analyzed the patterns of DNA−DNA photo-cross-linking. The results show that, when the cross-linker is on either the incoming or the recipient strand, it cross-links primarily to the outgoing strand. The cross-linker on the outgoing strand did not cross-link to any strand. This negative result can be explained if

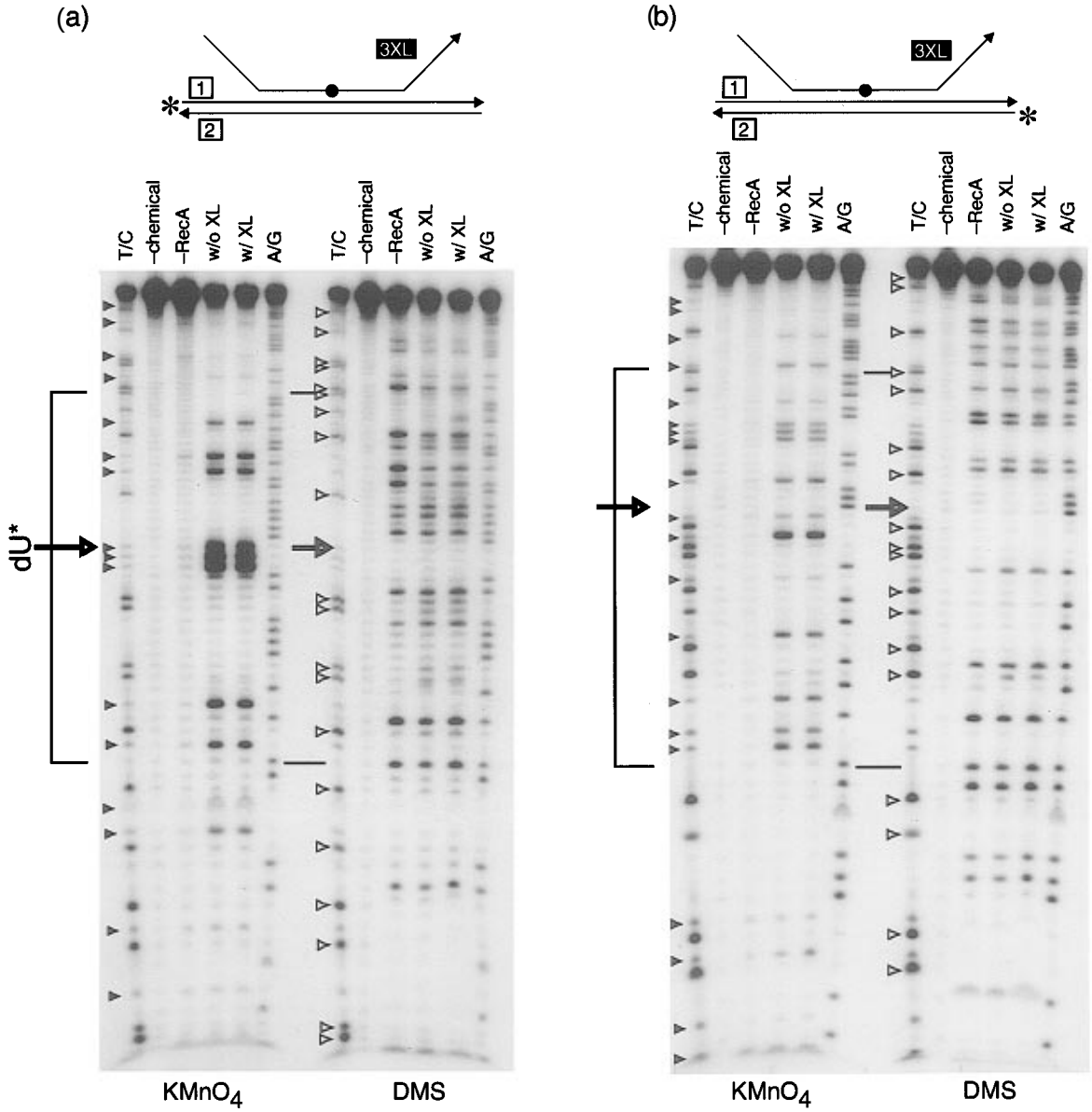

FIGURE 6: Chemical probing analyses of the synaptic complex made with photo-reactive incoming strand. The substrate combinations are shown at the top of each panel. The substrates in panel a and panel b differ only in the placement of [^{32}P] label. (a) Chemical reactivity patterns of the outgoing strand. The chemical used ($KMnO_4$ or DMS) is indicated at the bottom. Lanes, from left to right: Maxam−Gilbert T+C sequencing ladder (labeled "T/C"); control reaction without $KMnO_4$/DMS (− chemical); control reaction without RecA (− RecA); reactivity pattern of the synaptic complex involving non-photo-reactive oligo 3 as the incoming strand (w/o XL); reactivity pattern of the synaptic complex involving photo-reactive oligo 3XL as the incoming strand (w/XL); and Maxam−Gilbert A+G sequencing ladder (A/G). The region of homology is indicated by a bracket; a position corresponding to the dU* residue is indicated by a thick arrow. In the $KMnO_4$ column, filled arrowheads indicate locations of T residues; in the DMS column, open arrowheads indicate locations of C residues. (b) Chemical reactivity patterns of the recipient strand. Labels and symbols are identical to those in panel a.

the cross-linker on the outgoing strand is not pointing toward the hybrid duplex molecule, although this is not the only interpretation. In the second series of experiments, we treated the complex with DMS or $KMnO_4$ whose reactivity toward DNA bases depends on the base-pairing status. We compared the reactivity patterns between the synaptic complex made with a photo-reactive oligo and the one made without. The aim was to verify that the photo-cross-linking patterns obtained above represent a reaction stage after exchange of DNA strands, not before. The results show that the chemical reactivity patterns of the complex involving a photo-reactive oligo are identical to those derived from the complex lacking any photo-reactive oligo, even at or very near the position of dU*. These reactivity patterns are those of the products of strand exchange (Adzuma, 1992).

By combining the results of both series of experiments together, we conclude that, within the synaptic complex, the outgoing strand sits in the major groove of the hybrid duplex product. Our conclusion is based on two major assumptions concerning the conformation of DNA bases in the synaptic complex. First, we assume that DNA bases in the synaptic complex are oriented more or less perpendicular to the helical axis of DNA. This assumption has strong experimental support (Chabbert et al., 1991; Kubista et al., 1990; Takahashi et al., 1989). We also assume that the base conformation is "*anti*" as in B-DNA, not "*syn*"; i.e., bases are not flipped by 180°. This assumption seems reasonable but is tentative.

Our results argue against certain other possibilities for the strand arrangement within the synaptic complex. First, our

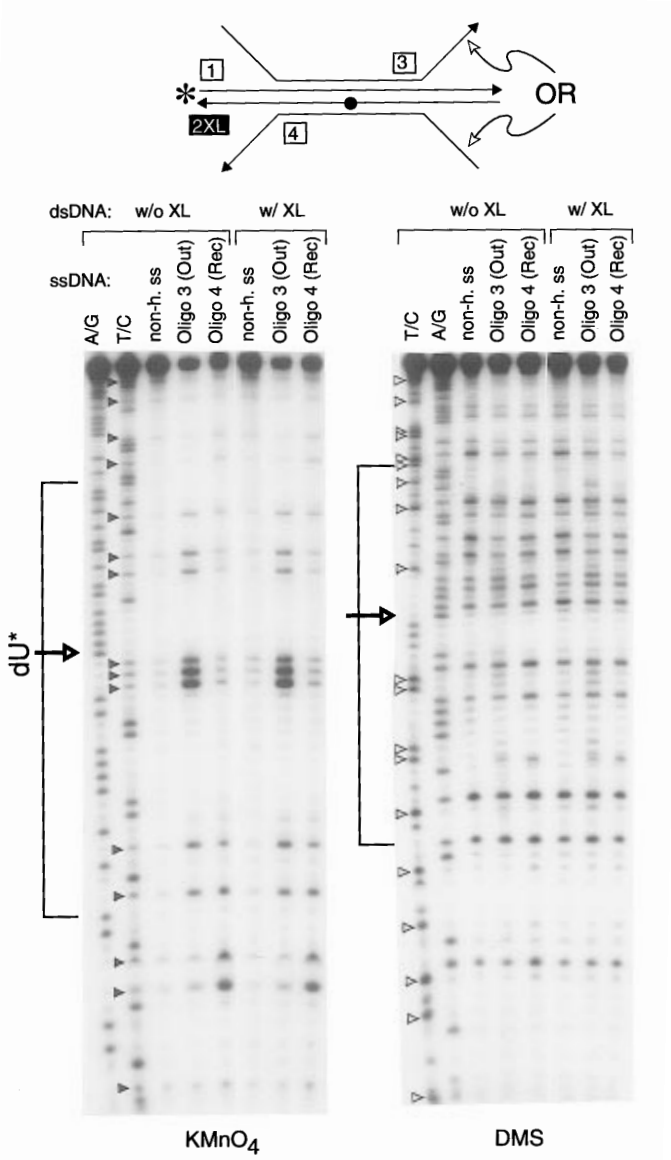

FIGURE 7: Chemical probing analyses of the synaptic complex made with photo-reactive dsDNA target. Symbols are the same as in Figure 6. The substrate combinations used are shown at the top. The dsDNA substrate was either a photo-reactive duplex (oligo 1/oligo 2XL; w/XL) or a non-photo-reactive control duplex (oligo 1/oligo 2; w/o XL). The ssDNA substrate was non-homologous ssDNA (non-h. ss), oligo 3, or oligo 4. In the presence of oligo 3 as the incoming strand, the [^{32}P]-labeled strand of the dsDNA substrate functioned as the outgoing strand ("Out"); in the presence of oligo 4, it functioned as the recipient strand ("Rec").

results argue against the idea that the outgoing strand sits in the minor groove of the hybrid duplex product. This point is not trivial, because the cross-linker used in this study, while attached to the major-groove edge of the base, nonetheless carries a long and flexible linker. By bending over and around the sugar−phosphate backbone, the photo-reactive group might be able to reach a region close to the minor groove. But our results demonstrate that a cross-linker on either the incoming or recipient strand, not just one of them, can cross-link to the outgoing strand. It is not easy to place the outgoing strand in the minor-groove side of the hybrid duplex molecule in such a way that this strand still remains accessible to a cross-linker conjugated to either strand of the hybrid duplex molecule. Second, our results argue against the idea of a stable, pre-exchange triplex in which the incoming strand is stably paired with an intact dsDNA via non-Watson−Crick hydrogen bonds. If such a triplex existed (see Figure 1; imagine that the incoming strand is connected to the major groove of the dsDNA target before exchange), then a cross-linker on the recipient strand should not be able to cross-link to the outgoing strand because the incoming strand would block it. On the contrary, we found that cross-linking between the recipient and outgoing strands occurs much more efficiently in the synaptic complex than in a simple dsDNA composed of just these two strands.

Two other groups reached the same conclusion as this study. Using an oligo tethered to iron−EDTA as an incoming strand, Baliga et al. (1995) examined the hydroxyl-radical cleavage patterns of a dsDNA target within the synaptic complex. The authors observed that the patterns did not agree with the existence of a stable pre-exchange triplex. The patterns were instead consistent with the view that the incoming strand invades the minor groove of the original dsDNA target, locally displacing the outgoing strand into the major groove of the hybrid duplex molecule. We also note in the results of Baliga et al. (1995) that the cleavage on the recipient strand was confined to within a few bases of a position corresponding to the EDTA-modified base, whereas some cleavages on the outgoing strand was as far as 13 nucleotides away. If the DNA strands within the synaptic complex maintain an axial base−base separation similar to canonical dsDNA−RecA−ATPγS complexes (5.1 Å; Egelman & Stasiak, 1986), 13 nucleotides would span a distance of 66 Å. Since it is highly unlikely that the hydroxyl radical could diffuse over such a long distance, the results imply that the outgoing strand may be mobile along the axis of the synaptic complex. Podyminogin et al. (1995) have analyzed the DNA structure within the synaptic complex using an oligo tethered with chlorambucil, a nitrogen mustard derivative which attacks mainly the N-7 of G. The resulting DNA−DNA chemical cross-linking patterns again strongly support the idea that the outgoing strand sits in the major groove of the hybrid duplex product. The authors observed no evidence for a stable, pre-exchange triplex. Interestingly, Podyminogin et al. (1995) also observed that the target bases of cross-linking were broadly distributed in the outgoing strand, implying a positionally unfixed nature of the outgoing strand within the synaptic complex. As pointed out by Podyminogin et al. (1995), these observations tend to speak against the existence of not only a pre-exchange triplex but also a post-exchange triplex proposed by Chiu et al. (1993).

In all, three independent groups using three different methods, i.e., iron−EDTA-induced affinity cleavage (Baliga et al., 1995), chlorambucil-driven chemical cross-linking (Podyminogin et al., 1995), and arylazido-driven photo-cross-linking (this study), all reached the same conclusion. Moreover, these three studies complement each other's weakness. For example, we examined the behavior of all three DNA strands, whereas the other two groups placed the reporter group only on the incoming strand; on the other hand, our experiments do not precisely determine the location of cross-linking, whereas the other two studies mapped the sites of cleavage or cross-linking at the nucleotide level.

Strand Invasion Occurs in the Minor Groove of a dsDNA Target. To the approaching ssDNA−RecA presynaptic complex, each groove of a dsDNA target would expose a chemical environment distinct from the other groove. Thus depending on the target groove, the mechanics for strand

invasion would have to differ. Unless dual mechanics is built-in to RecA, the two models for strand invasion should be mutually exclusive.

We have shown that, after local strand exchange, the outgoing strand sits in the major-groove side of the hybrid duplex product. This post-exchange arrangement of DNA strands strongly indicates that, before exchange, strand invasion occurs in the minor groove of the original dsDNA substrate (see Figure 1). If the strand invasion had occurred in the major groove of a target dsDNA, the outgoing strand would have been "pushed" into the minor-groove side of the hybrid duplex.

Is it possible that, after strand exchange, the displaced outgoing strand might translocate from the minor groove to the major groove? Our results alone do not rule out this possibility. However, there is no obvious mechanistic reason why such a relocation should occur as an obligatory reaction step. Undoing the DNA synapsis would also be awkward in this case. To reverse the synapsis, which might take place repeatedly during the homology search phase, the outgoing strand this time would have to turn 180° back to the original minor-groove side of the hybrid duplex, in order to be consistent with the principle of microscopic reversibility.

Another possibility might be that the outgoing strand, after being displaced into the minor groove, becomes highly mobile in the synaptic complex, moving back and forth between the two grooves. Photo-cross-linking might have just selected a population of the outgoing strand molecules which happened to be in the major groove at the time of UV irradiation. However, such movement would be difficult within RecA filaments. In dsDNA−RecA−ATPγS filaments, DNA molecules are axially stretched to such an extent (50% longer than B-DNA) that the furthest possible cross-axial distance of travel of a resident DNA strand is calculated to be about 17 Å (Egelman & Stasiak, 1986). That is, the resident DNA strands on average cannot go beyond this distance without breaking the DNA strand. A ssDNA strand within ssDNA−RecA−ATPγS filaments also shows a stretched configuration (Yu & Egelman, 1992). Assuming that these helical parameters of DNA strands are conserved also in the synaptic complex, the three DNA strands in the synaptic complex would be confined within a virtual cylinder of less than 17 Å in radius. This confinement of three DNA strands is very "crowded", and it would be difficult for the locally displaced strand to freely move back and forth between the two grooves of the hybrid duplex molecule. We also point out that this calculated maximum for the radius of DNA strands within RecA filaments, 17 Å, is only one-third of the actual radius of the RecA filament itself (∼50 Å). This means that a "displaced" strand would not be able to escape the synaptic complex even without any stable contacts with RecA or with the hybrid duplex product, unless it has a free end.

Implication of the Minor Groove Invasion Model. The idea of the minor-groove invasion has two implications. Firstly, it does not support the triplex model for homology recognition, to the extent that this model relies on homology recognition taking place in the major groove of a dsDNA target. Secondly, it is consistent with the melting−annealing model for homology recognition. We do not totally discount the possibility that weak interactions might exist between an incoming ssDNA strand and the minor groove of the dsDNA target. However, such an interaction in the minor groove, if any, would probably be incapable of distinguishing all four base pairs.

A major reason why the melting−annealing model has not gained greater acceptance is the well-established observation that RecA exhibits no straightforward strand-separation activity like DNA helicases, even in the presence of ATP (Hsieh & Camerini-Otero, 1989; West et al., 1981; Wu et al., 1983). This lack of strand-separation activity, however, should not be taken as evidence against the melting−annealing model, because this model does not require complete separation of DNA strands. To read the sequence of the target dsDNA by a melting−annealing mechanism, the presynaptic complex only needs to shift the internal equilibrium between paired and unpaired states of base pairs toward the unpaired state. There is no need for the complex to completely separate the two strands as DNA helicases do. RecA might promote the transient opening of base pairs just by stretching the DNA strands, i.e., by disrupting the base-stacking interaction which contributes significantly to the stability of dsDNA molecules. Moreover, if transient opening occurs, for instance, only 10% on a time-averaged basis, it might not be easy to detect such opening by conventional means such as chemical probing.

Finally, modification of the C-5 of uracil with our bulky photo-cross-linker had no effect on the local strand exchange. This might have a pharmaceutical application. One can easily attach various groups to the pyrimidine C-5 and chances are good that such modification would have no detrimental effect on the recombination in vivo. It is interesting to note here that genomic DNA of T-even bacteriophages is already heavily glycosylated at the cytosine C-5, but recombination does occur efficiently in those phages.

ACKNOWLEDGMENT

We are grateful to Dr. Peter Model (Rockefeller University), Drs. Kiyoshi Mizuuchi and Robert Craigie (National Institutes of Health), and Dr. Howard Gamper (Epoch Pharmaceuticals, Inc.) for critical reading of the manuscript.

REFERENCES

Adzuma, K. (1992) *Genes Dev. 6*, 1679−1694.
Baliga, R., Singleton, J. W., & Dervan, P. B. (1995) *Proc. Natl. Acad. Sci. U.S.A. 92*, 10393−10397.
Beal, P. A., & Dervan, P. B. (1991) *Science 251*, 1360−1363.
Camerini-Otero, R. D., & Hsieh, P. (1993) *Cell 73*, 217−223.
Chabbert, M., Lami, H., & Takahashi, M. (1991) *J. Biol. Chem. 266*, 5395−5400.
Chiu, S. K., Rao, B. J., Story, R. M., & Radding, C. M. (1993) *Biochemistry 32*, 13146−13155.
Cotterill, S. M., Satterthwait, A. C., & Fersht, A. R. (1982) *Biochemistry 21*, 4332−4337.
Cowing, D. W., Mecsas, J., Record, M. T., Jr., & Gross, C. A. (1989) *J. Mol. Biol. 210*, 521−530.
Cox, M. M. (1994) *Trends Biochem. Sci. 19*, 217−222.
Cox, M. M. (1995) *J. Biol. Chem. 270*, 26021−26024.
Egelman, E. H., & Stasiak, A. (1986) *J. Mol. Biol. 191*, 677−697.
Frank-Kamenetskii, M. D., & Mirkin, S. M. (1995) *Annu. Rev. Biochem. 64*, 65−95.
Honigberg, S. M., Gonda, D. K., Flory, J., & Radding, C. M. (1985) *J. Biol. Chem. 260*, 11845−11851.
Hsieh, P., & Camerini-Otero, R. D. (1989) *J. Biol. Chem. 264*, 5089−5097.
Hsieh, P., Camerini-Otero, C. S., & Camerini-Otero, R. D. (1990) *Genes Dev. 4*, 1951−1963.

Iida, S., & Hayatsu, H. (1971) *Biochem. Biophys. Acta. 240*, 370−375.
Jain, S. K., Cox, M. M., & Inman, R. B. (1995) *J. Biol. Chem. 270*, 4943−4949.
Kowalczykowski, S. (1991) *Annu. Rev. Biophys. Biophys. Chem. 20*, 539−575.
Kowalczykowski, S., & Eggleston, A. (1994) *Annu. Rev. Biochem. 63*, 991−1043.
Kubista, M., Takahashi, M., & Norden, B. (1990) *J. Biol. Chem. 265*, 18891−18897.
Kuramitsu, S., Hamaguchi, K., Ogawa, T., & Ogawa, H. (1981) *J. Biochem. (Tokyo) 90*, 1033−1045.
Lewis, R. V., Roberts, M. F., Dennis, E. A., & Allison, W. S. (1977) *Biochemistry 16*, 5650−5654.
Maxam, A. M., & Gilbert, W. (1980) *Methods Enzymol. 65*, 499−560.
Menetski, J. P., Bear, D. G., & Kowalczykowski, S. C. (1990) *Proc. Natl. Acad. Sci. U.S.A. 87*, 21−25.
Moser, H. E., & Dervan, P. B. (1987) *Science 238*, 645−650.
Podyminogin, M. A., Meyer, R. B., & Gamper, H. B. (1995) *Biochemistry 34*, 13098−13108.
Rao, B. J., & Radding, C. M. (1994) *Proc. Natl. Acad. Sci. U.S.A. 91*, 6161−6165.
Rao, B. J., Dutreix, M., & Radding, C. M. (1991) *Proc. Natl. Acad. Sci. U.S.A. 88*, 2984−2988.
Rao, B. J., Chiu, S. K., & Radding, C. M. (1993) *J. Mol. Biol. 229*, 328−343.
Roca, A. I., & Cox, M. M. (1990) *Crit. Rev. Biochem. Mol. Biol. 25*, 415−456.
Shchyolkina, A. K., Timofeev, E. N., Borisova, O. F., Il'icheva, I. A., Minyat, E. E., Khomyakova, E. B., & Florentiev, V. L. (1994) *FEBS Lett. 339*, 113−118.
Shinohara, A., Ogawa, H., Matsuda, Y., Ushio, N., Ikeo, K., & Ogawa, T. (1993) *Nat. Genet. 4*, 239−243.
Stasiak, A. (1992) *Mol. Microbiol. 6*, 3267−3276.
Takahashi, M., Kubista, M., & Norden, B. (1989) *J. Mol. Biol. 205*, 137−147.
Tsang, S. S., Muniyappa, K., Azhderian, E., Gonda, D. K., Radding, C. M., Flory, J., & Chase, J. W. (1985) *J. Mol. Biol. 185*, 295−309.
Uhlin, B. E., & Clark, A. J. (1981) *J. Bacteriol. 148*, 386−390.
West, S. C. (1992) *Annu. Rev. Biochem. 61*, 603−640.
West, S. C., Cassuto, E., & Howard-Flanders, P. (1981) *Nature 290*, 29−33.
Wu, A. M., Bianchi, M., DasGupta, C., & Radding, C. M. (1983) *Proc. Natl. Acad. Sci. U.S.A. 80*, 1256−1260.
Yoshimura, Y., Morita, T., Yamamoto, A., & Matsushiro, A. (1993) *Nucleic Acids Res. 21*, 1665.
Yu, X., & Egelman, E. (1992) *J. Mol. Biol. 227*, 334−346.
Zhurkin, V. B., Raghunathan, G., Ulyanov, N. B., Camerini-Otero, R. D., & Jernigan, R. L. (1994) *J. Mol. Biol. 239*, 181−200.

BI9630063